PROCEEDINGS OF SCIENCE

Observation and study of B meson decays with Λ_c baryons with the *BABAR* detector

Thomas Hartmann (For the *BABAR* Collaboration)∗†
University of Rostock
Universitätsplatz 3
D-18051 Rostock (Germany)
http://topas.physik2.uni-rostock.de/~hartmann/
E-mail: thomas.hartmann@uni-rostock.de

We present results and interpretations of studies of B meson decays into final states with baryons based on 467×10^6 $B\bar{B}$ pairs taken with the *BABAR* detector. The study of $\bar{B}^0 \to \Lambda_c^+ \overline{p}\pi^0$ ‡ is presented and compared to the isospin-related decay $B^- \to \Lambda_c^+ \overline{p}\pi^-$ [1]. Furthermore, relations between baryonic decays with respect to Cabibbo-suppression, multiplicity relations and substructures in the invariant baryon-antibaryon invariant masses are shown. In addition interpretations of the mechanisms behind baryonic B meson decays are discussed.

35th International Conference of High Energy Physics - ICHEP2010,
July 22-28, 2010
Paris France

∗Speaker.
†Many thanks to all colleagues at *BABAR* and PEP-II
‡Charge conjugation is implied if not stated otherwise

1. Introduction

Decays of heavy mesons into final states with a baryon-antibaryon pair show characteristics distinct from pure mesonic decays. Studies on the large dataset of $426\,\mathrm{fb}^{-1}$ equivalent to 467×10^6 $B\bar{B}$ pairs taken with the BABAR detector can lead to an understanding of decays with baryonic final states. B mesons are well suited for such studies since $(6.8 \pm 0.6)\,\%$ of all B mesons decay into baryons [2]; yet, to date, only about one seventh of all baryonic B decays branching fractions have been measured exclusively. Furthermore, the processes of hadronization into baryonic final states lack a profound understanding.

2. Study of $\bar{B}^0 \to \Lambda_c^+ \overline{p} \pi^0$ [3]

Based on a dataset of $2.39\,\mathrm{fb}^{-1}$, CLEO measured an upper limit $\mathscr{B}\left(\bar{B}^0 \to \Lambda_c^+ \overline{p} \pi^0\right) < 5.9 \cdot 10^{-4}$ [4]. Based on the complete dataset, BABAR has now measured a branching fraction $\mathscr{B}\left(\bar{B}^0 \to \Lambda_c^+ \overline{p} \pi^0\right) = \left(1.94 \pm 0.17_{\mathrm{stat}} \pm 0.14_{\mathrm{sys}} \pm 0.50_{\Lambda_c}\right) \times 10^{-4}$ [3], where the uncertainties are statistical, systematic and due to the uncertainty on the branching fraction $\mathscr{B}\left(\Lambda_c^+ \to pK^-\pi^+\right) = (5.0 \pm 1.3) \cdot 10^{-2}$ [5].
The decay is reconstructed in the decay chain $\bar{B}^0 \to \Lambda_c^+ \overline{p} \pi^0$; $\Lambda_c^+ \to pK^-\pi^+$; $\pi^0 \to \gamma\gamma$. Charged final state particles are reconstructed using tracking and particle ID from the BABAR sub-detectors. Photons are reconstructed in showers in the electromagnetic calorimeter. To reduce background a cut on the event topology is required, which discriminates the event shapes of continuum events against B events. Cuts on $m(\gamma\gamma)$ and $m(pK^-\pi^+)$ are applied to select π^0 and Λ_c^+ candidates. The Λ_c^+ and π^0 candidates are combined with a $\overline{p}$ to form a $\bar{B}^0$ candidate. Cuts on the vertex fit qualities for the Λ_c^+ and $\bar{B}^0$ candidates further reduce combinatorial background. In about 10% of the events multiple B candidates are reconstructed; one unique candidate is selected based on the mass differences from the nominal masses for the reconstructed $m(\gamma\gamma)$ and $m(pK^-\pi^+)$, and the B vertex fit quality.

$\bar{B}^0$ candidates can be reconstructed in the e^+e^- center-of-mass frame in two nearly independent kinematic variables $m_{\mathrm{ES}} = \sqrt{\left(\frac{s}{2} + \mathbf{p}_0 \cdot \mathbf{p}_B / E_0\right)^2 - \mathbf{p}_B^2}$ and $\Delta E = E_B^* - \frac{\sqrt{s}}{2}$, where $(E_B^*, \mathbf{p}_B)$ is the reconstructed B four-momentum in the laboratory frame and $(E_0, \mathbf{p}_0)$ is the e^+e^- four-momentum. In this analysis ΔE was used to suppress similar B decays with higher and lower multiplicities. Peaking background arises from events from the isospin-related decay $B^- \to \Lambda_c^+ \overline{p} \pi^-$ and in particular the resonant decay $B^- \to \Sigma_c^0(2455)\overline{p}$. If such a candidate is reconstructed lying in the m_{ES} and ΔE signal range or around the $\Sigma_c^0(2455)$ invariant mass, the whole event is rejected.
In m_{ES} the signal shape is fitted with the sum of two Gaussians and the background with an ARGUS function [6]. 273 ± 23 events are observed with a significance of $> 10\sigma$ (Fig. 1). To take discrepancies between MC and data into account, the efficiency is corrected along the invariant mass $m\left(\Lambda_c^+ \pi^0\right)$. An efficiency function is fitted to bins of $m\left(\Lambda_c^+ \pi^0\right)$ from MC. Each data event is then weighted by the inverse of the fitted efficiency function. In the corrected m_{ES} distribution 4528 ± 403 events are observed.
The main sources of systematic uncertainty is the discrepancy between the MC model and real data, which is about 5.1%.

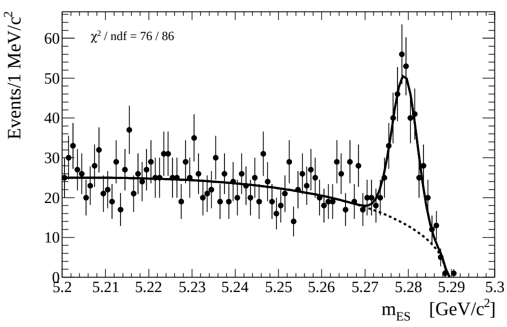

Figure 1: $\bar{B}^0 \to \Lambda_c^+ \overline{p} \pi^0$:$m_{\mathrm{ES}}$ distribution after applying all constraints without efficiency correction.

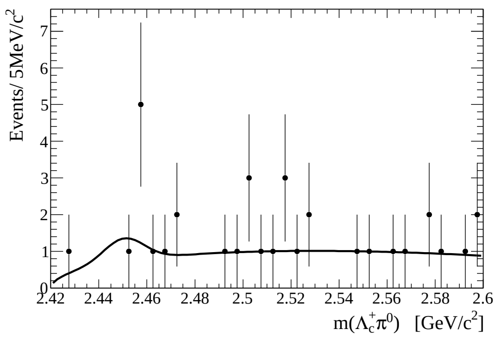

Figure 2: $\bar{B}^0 \to \left(\Lambda_c^+ \pi^0\right) \overline{p}$: Search for Σ_c^+ resonances.

2.1 $\bar{B}^0 \to \Sigma_c^+(2455)\overline{p}$ search

Various intermediate states with resonances are known from similar baryonic B decays [1, 7, 8, 9]. For $\bar{B}^0 \to \Lambda_c^+ \overline{p} \pi^0$ intermediate states with Σ_c^+ resonances are searched for in the invariant mass $m\left(\Lambda_c^+ \pi^0\right)$; as shown in figure 2 no evidence for an intermediate state with a Σ_c^+ (2455) resonance is found. The fit to $m\left(\Lambda_c^+ \pi^0\right)$ returns 3 ± 3 signal events and a Bayesian upper limit at 90% C.L. of $\mathscr{B}\left(\bar{B}^0 \to \Sigma_c^+(2455)\overline{p}\right) \times \mathscr{B}\left(\Lambda_c^+ \to pK^-\pi^+\right) < 1.5 \times 10^{-6}$ is obtained.

3. Properties of baryonic B decays

To some extent B decays with baryonic final states show differences to pure mesonic or semileptonic decays. For example decay dynamics of baryonic decays show interesting features, which are not common to mesonic decays.

3.1 Multiplicity dependence

Similar to mesonic decays, e.g. decays $D^\pm \to K(\mathsf{n} \cdot \pi)$, B decays into baryonic final states show an increase of the branching fraction with the multiplicity. For example, the branching fractions increase by factors of 10-13 from the two-body final state to the three body final states $B \to \Lambda_c^+ \overline{p}(\mathsf{n} \cdot \pi)$ with $\mathsf{n} = 0 \to 1$. For $\mathsf{n} = 1 \to 2$ and $\mathsf{n} = 2 \to 3$ the increases of the branching fractions are between factors of 2-4 [3, 1, 8, 9]. Similar, for the decays with the minimal three-body final states $B \to D^{(*)} p\overline{p}(\mathsf{n} \cdot \pi)$ the increases in the branching fractions with $\mathsf{n} = 0 \to 1$ are between $\sim 3 - 4.5$ [10].

For $B \to D^{(*)} p\overline{p}(\mathsf{n} \cdot \pi)$ with $\mathsf{n} = 1 \to 2$ the branching ratios start to decrease, while for $B \to \Lambda_c^+ \overline{p}(\mathsf{n} \cdot \pi)$ no decrease has been seen up to $\mathsf{n} = 2 \to 3$.

This suggests that decays to states with only a baryon-antibaryon pair are not favored.

3.2 Isospin comparison $\frac{\Gamma\left(\bar{B}^0 \to \Lambda_c^+ \overline{p} \pi^0\right)}{\Gamma\left(B^- \to \Lambda_c^+ \overline{p} \pi^-\right)}$

While for $\bar{B}^0 \to \Lambda_c^+ \overline{p} \pi^0$ two isospin states $I = \frac{1}{2}$ or $I = \frac{3}{2}$ are possible, for the isospin-related decay $B^- \to \Lambda_c^+ \overline{p} \pi^-$ only $I = \frac{3}{2}$ is possible [1]. If one assumes only major contributions from $I = \frac{3}{2}$ states, a ratio of the partial decay widths of $\frac{\Gamma\left(\bar{B}^0 \to \Lambda_c^+ \overline{p} \pi^0\right)}{\Gamma\left(B^- \to \Lambda_c^+ \overline{p} \pi^-\right)} = \frac{2}{3}$ is expected. If however due to

some unknown reason decay amplitudes contributing to $\bar{B}^0 \to \Lambda_c^+ \overline{p} \pi^0$ with $I = \frac{1}{2}$ would dominate, like a W^- exchange between the two B constituent quarks, a deviation from the expectation would be visible.
The measured ratios

$$\frac{\Gamma\left(\bar{B}^0 \to \Lambda_c^+ \overline{p} \pi^0\right)}{\Gamma\left(B^- \to \Lambda_c^+ \overline{p} \pi^-\right)} = 0.61 \pm 0.09 \quad , \quad \frac{\Gamma\left(\bar{B}^0 \to \Lambda_c^+ \overline{p} \pi^0\right)}{\Gamma\left(B^- \to \Lambda_c^+ \overline{p} \pi^-\right)_{\text{non-resonant}}} = 0.80 \pm 0.11$$

with the total $\mathscr{B}(B^- \to \Lambda_c^+ \overline{p} \pi^-)$ as well as only the non-resonant branching ratio without Σ_c^0 intermediate states are both compatible with the expectation within the uncertainties. Apparently, both decays are dominated by decay amplitudes with $I = \frac{3}{2}$.

3.3 Cabibbo suppression

Furthermore, contributing decay amplitudes and processes can be compared with respect to a Cabibbo suppression. While the decay $\bar{B}^0 \to \Lambda_c^+ \overline{p} \pi^+ \pi^-$ [8] is Cabibbo favored the decay $\bar{B}^0 \to \Lambda_c^+ \overline{p} K^- \pi^+$ is suppressed [7]. The same holds true for the resonant intermediate states $\bar{B}^0 \to \Sigma_c^{++}(2455) \overline{p} \pi^-$ and $\bar{B}^0 \to \Sigma_c^{++}(2455) \overline{p} K^-$.
The measured branching fraction ratios of the resonant and non-resonant decays are

$$\frac{\Gamma\left(\bar{B}^0 \to \Lambda_c^+ \overline{p} K^- \pi^+\right)}{\Gamma\left(\bar{B}^0 \to \Lambda_c^+ \overline{p} \pi^- \pi^+\right)} = 0.038 \pm 0.009 \quad , \quad \frac{\Gamma\left(\bar{B}^0 \to \Sigma_c^{++}(2455) \overline{p} K^-\right)}{\Gamma\left(\bar{B}^0 \to \Sigma_c^{++}(2455) \overline{p} \pi^-\right)} = 0.048 \pm 0.016$$

Both ratios are compatible with the Cabibbo angle $\left|\frac{V_{us}}{V_{ud}}\right|^2 = 0.054 \pm 0.002$ [5] within 2σ. Although the smaller ratio of the four body final states suggests that additional decay amplitudes in the Cabibbo favored decay are not negligible, as for example intermediate states with Σ_c^0 resonances, which are only possible for $\bar{B}^0 \to \Lambda_c^+ \overline{p} \pi^- \pi^+$.

3.4 Baryon-antibaryon threshold enhancement

For signal events of the decay $\bar{B}^0 \to \Lambda_c^+ \overline{p} \pi^0$ a discrepancy between data and MC at the threshold in the baryon-antibaryon distribution $m(\Lambda_c^+ \overline{p})$ is visible at 5σ significance (Fig. 3).
Also in various other decays to baryonic final states an enhancement near the baryon-antibaryon threshold is seen which is not compatible with a simple phase space model. Such enhancements were measured in B decays with charmed baryons, e.g. $B^- \to \Lambda_c^+ \overline{p} \pi^-$ [1], in B decays with charmed mesons e.g. $\bar{B}^0 \to D^0 p \overline{p}$ [10], in charmless B decays, e.g. $B^- \to \overline{\Lambda} p \pi^-$ (Fig. 4) [11] as well as in other processes, e.g. $e^+e^- \to \gamma \Lambda \overline{\Lambda}$ [12].
Since in mesonic decays such a distinct behavior has not been seen, it seems to be a special feature of baryonic decays.

4. Phenomenological hadronization model interpretation

A few suggestions were made to explain these phenomena in baryonic decays [13, 14].
Hypotheses on the nature of baryon decays differ for example in assuming either short-distance or long-distance production mechanisms. In a short-distance argument the hadronization proceeds

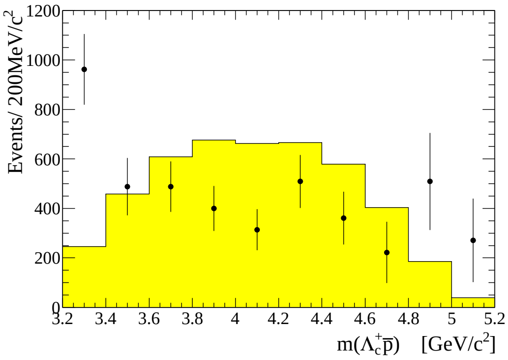

Figure 3: $\bar{B}^0 \to \Lambda_c^+ \overline{p} \pi^0$: $m\left(\Lambda_c^+ \overline{p}\right)$ distribution data: points with error bars; MC: histogram.

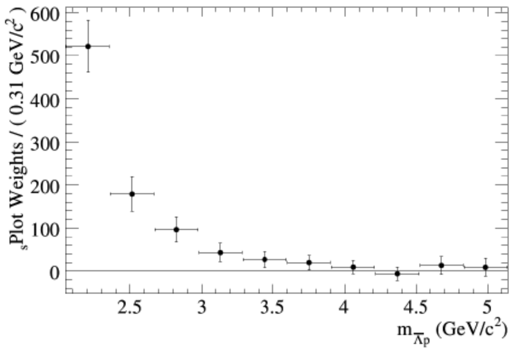

Figure 4: $B^- \to \overline{\Lambda} p \pi^-$: $m\left(\overline{\Lambda} p\right)$ distribution.

via an initial hard gluon producing a $q\overline{q}$ pair back-to-back with high q^2, so that the initial *diquark-antidiquark* pair forms the primary baryon-antibaryon pair. Since the baryon-antibaryon pair is aligned back-to-back no enhancement in the baryon-antibaryon invariant mass is expected in such a production mechanism. In this picture further mesons in the final states would be produced from the hadronization of one or both initial baryons (Fig. 5a).

In contrast in a long-distance model the final state contains at least three particles. Here, the initial state is a *meson meson-like* state where the meson-like state further hadronizes into the baryon-antibaryon pair. So, the gluon is near to the mass shell of the *meson-like* $q\overline{q}$ pair with a low q^2 value (for example, Fig. 5b,c,d). One interpretation for the *meson-like* states would be virtual mesons at typical masses $(D, \eta, \cdots)$, which are below the baryon-antibaryon threshold. Also from another perspective, roughly speaking, the emitted real meson condenses the remaining $q\overline{q}$ pair into a smaller phase space and enhances the probability of a baryon-antibaryon formation. Subsequently, a smaller baryon-antibaryon invariant mass can be expected as well as higher multiplicity final states.

For example, the resonant decay $\bar{B}^0 \to \Sigma_c^0(2455)\overline{p}\pi^+$ is suppressed to $\bar{B}^0 \to \Sigma_c^{++}(2455)\overline{p}\pi^-$ by $\frac{\bar{B}^0 \to \Sigma_c^0(2455)\overline{p}\pi^+}{\bar{B}^0 \to \Sigma_c^{++}(2455)\overline{p}\pi^-} = 0.57 \pm 0.27$ [8]. Since the decay $\bar{B}^0 \to \Sigma_c^0(2455)\overline{p}\pi^+$ can only proceed via an initial *diquark-antidiquark* state one would also expect no threshold enhancement in the $m\left(\Sigma_c^0(2455)\overline{p}\right)$ invariant mass. In contrast, *diquark-antidiquark* and *meson meson-like* decay amplitudes can contribute to $\bar{B}^0 \to \Sigma_c^{++}(2455)\overline{p}\pi^-$. Consequently, a larger branching fraction seems natural and one also would expect a threshold enhancement in the $m\left(\Sigma_c^{++}(2455)\overline{p}\right)$ invariant mass.

References

[1] BABAR Collab. (B. Aubert *et al.*), Phys. Rev. D78, 112003 (2008)

[2] ARGUS Collab. (H. Albrecht *et al.*), Z. Phys., C 56, 1 (1992)

[3] BABAR Collab. (B. Aubert *et al.*), Phys. Rev. D82, 031102 (2010)

[4] CLEO Collab. (Fu, X. *et al.*), Phys. Rev. Lett. 79, 3125 (1997)

[5] Particle Data Group (Amsler, C. *et al.*) Phys. Lett. B667 (2008)

[6] ARGUS Collab. (Albrecht, H. *et al.*), Phys. Lett. B241, 278 (1990)

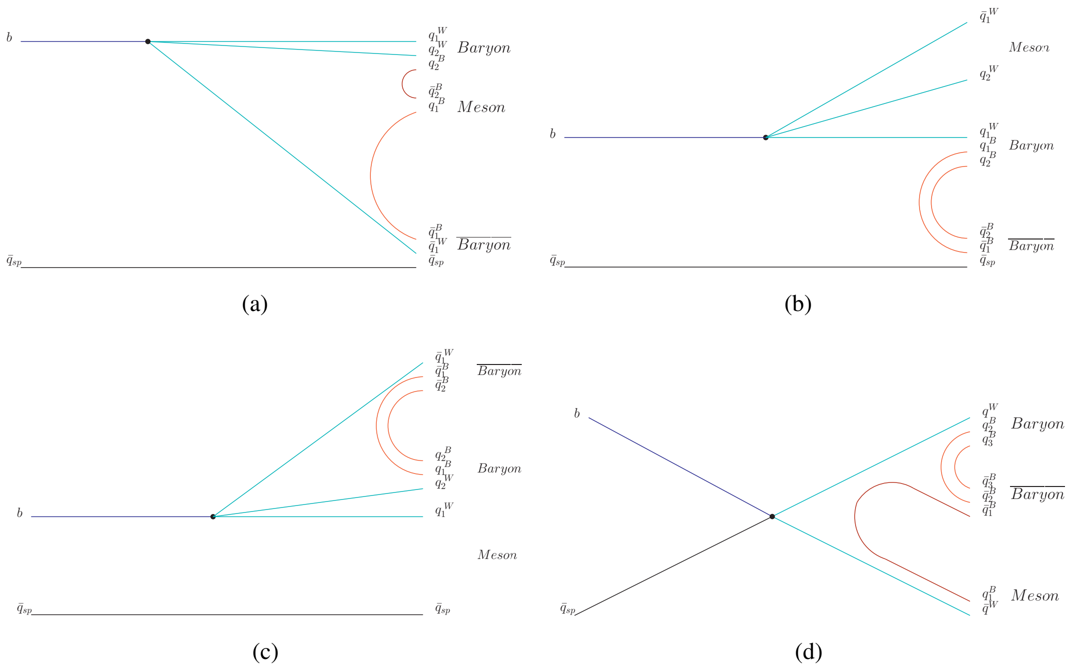

Figure 5: Baryonization diagrams: Selection of effective hadronization diagrams for B meson decays into a baryon-antibaryon pair plus one meson. Diagram (a) proceeds via an initial *diquark-antidiquark*, i.e. baryon-antibaryon, pair with the following hadronization of one of the baryons into the three body final state; the initial states in diagrams (b), (c), (d) are *meson meson-like* states with the baryonization of the *meson-like* $q\bar{q}$-pair into the three body final state.

[7] *BABAR* Collab. (B. Aubert *et al.*), Phys. Rev. D80, 051105 (2009)

[8] Belle Collab. (K. S. Park *et al.*), Phys. Rev. D75, 011101 (2007)

[9] CLEO Collab. (Dytman, S. A. *et al.*), Phys. Rev. D66, 091101 (2002)

[10] *BABAR* Collab. (B. Aubert *et al.*), hep-ex:0908.2202

[11] *BABAR* Collab. (B. Aubert *et al.*), Phys. Rev. D79, 112009 (2009)

[12] *BABAR* Collab. (B. Aubert *et al.*), Phys. Rev. D76, 092006 (2007)

[13] M. Suzuki, J.Phys. G34, 283 (2006)

[14] W. Hou and A. Soni Phys. Rev. Lett. 86, 4247 (2001)